JOURNAL OF MATERIALS SCIENCE **36** (2001) 5903–5907

Microstructural and magnetic studies on P/M processed $(Nd_{14.9}Dy_{1.9})(Fe_{65.0}Co_{8.0}Cu_{1.0}Ga_{1.0}Nb_{0.7})B_{7.5}$ alloy

S. PANDIAN, V. CHANDRASEKARAN
Defence Metallurgical Research Laboratory, Hyderabad 500 058, India

K. J. L. IYER, K. V. S. RAMA RAO
Indian Institute of Technology, Madras 600 036, India

Sintered samples of $(Nd_{14.9}\ Dy_{1.9})\ (Fe_{65}\ Co_8\ Cu_{1.0}\ Ga_{1.0}\ Nb_{0.7})B_{7.5}$ were prepared and subjected to stepwise annealing in the temperature range 875 K–675 K. The XRD and metallographic (optical and electron microscopy) studies reveal a multi-phase microstructure with each phase showing different solubility of the alloying additions. This alloy has T_C of 705 K with an intrinsic coercivity of 1000 kA/m and energy product of $\sim$250 kJ/m^3 at RT. Solubility of Co into the matrix phase and that of Ga and Cu into the Nd-rich grain boundary phase are considered to be the main contributing factors for the significant enhancement in T_C and H_{ci} respectively of the multi-component alloy when compared to those of ternary NdFeB, wherein $H_{ci} = 720$ kA/m and $T_C = 585$ K.

1. Introduction

Excellent permanent magnetic properties are exhibited by sintered Nd-Fe-B magnets with $Nd_2Fe_{14}B$ as major phase (φ-phase) and are exploited for enhancing the performance and/or reducing the size of many electrotechnical devices. However, owing to thermal instability of remanence (B_r) and intrinsic coercivity (H_{ci}) at elevated temperatures [1], limitations exist in the applicability of this class of permanent magnet material. The main interest of research has quite long been focussed on designing the alloy with suitable additions so that substantial improvement in the magnetocrystalline anisotropy field (H_A) and Curie temperature (T_C) of the φ-phase is achieved without much reduction in B_r. Substitution of Nd by Dy increases the anisotropy field of the φ-phase and has profound influence on the coercivity [2, 3]. However such substitutions bring down the magnetization owing to ferri-magnetic coupling of the heavy rare earths with 3d-elements (Fe, Co) and therefore Dy substitution is restricted only to a limited concentration level. Similarly, addition of Co in place of Fe results in the enhancement of T_C, but is accompanied by decrease in coercivity due to the formation of soft magnetic phases such as Nd $(FeCo)_2$ and Nd $(FeCo)_3$ [4, 5]. Even though the combined addition of Dy and Co appears to be an appropriate choice for the optimal balance of H_{ci} and T_C, suitable microstructural modifications are also needed to reduce its deteriorating influences. In ternary Nd-Fe-B, a Nd-rich eutectic phase acts as sintering aid liquid phase and helps in the magnetic isolation of the φ-phase grains by delineating the grain boundary [6]. This phase undergoes modification due to alloying additions. Additives such as Cu, Nb, Ga etc., were tried [7–9] to improve H_{ci} mainly with the intention to propitiate the microstructure with non-magnetic nature of the secondary phases and uniform distribution of them in the intergranular region. Thus, for optimal permanent magnetic properties, many combinations of alloying additions to NdFeB are being explored. It has been reported that Cu brings down the melting point of the sintering aid Nd-rich eutectic [7], but causes deterioration in coercivity due to precipitation of α-Fe particles [10]. The study by Liu *et al.* [11], on the other hand, indicated that Fe precipitation could be suppressed by the addition of Nb. The combined addition of Cu and Nb therefore will aid the development of a microstructure, conducive for coercivity enhancement. Further, Ga is considered as an important additive since high coercivity can be obtained through modification in the microstructure, while its solubility in the matrix phase at low concentration level is rather found to increase H_A and T_C marginally [12]. The simultaneous addition of Ga and Nb was found to be effective in getting very high coercivity without affecting the T_C of the matrix phase [13]. It is therefore interesting to study the effect of these three alloying additions viz Cu, Ga and Nb in combination with Dy and Co in the NdFeB system. Accordingly, alloy of (NdDy)(FeCoNbGaCu)B has been powder metallurgically processed and its microstructural features and the magnetic properties are reported in this paper. Studies on ternary NdFeB have also been made for comparison.

2. Experimental

NdFeB alloys of $Nd_{16.8}\ Fe_{75.7}B_{7.5}$ (alloy-1) and $(Nd_{14.9}Dy_{1.9})(Fe_{65}Co_{8.0}Cu_{1.0}Ga_{1.0}Nb_{0.7})B_{7.5}$ (alloy-2)

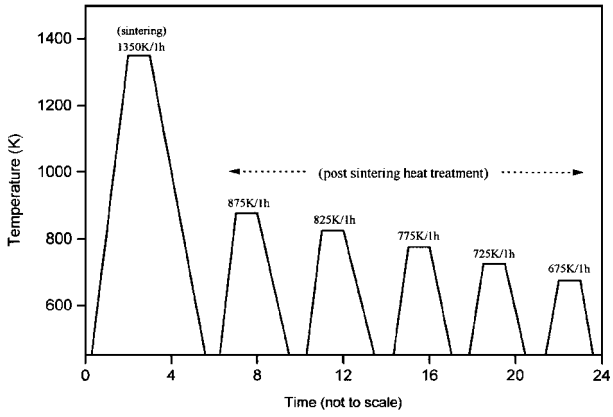

Figure 1 Thermal processing schedule adopted for sintering and post sintering heat treatment of samples 1 and 2.

were prepared by vacuum induction melting of the constituent elements. The alloy ingots were crushed and ball milled to fine powder of average particle size ~5 μm. The particles were magnetically oriented in the presence of an aligning magnetic field of >1.5 T and compacted into cylindrical test samples of 20 mm diameter and 10 mm height. They were sintered at 1350 K, followed by a multi-stage post-sintering heat treatment from 875 K to 675 K. A schematic of the thermal process schedule adopted is presented in Fig. 1. The room temperature permanent magnet characteristics of the fully heat-treated samples were evaluated using an auto-hysteresis graph. The temperature variation of magnetization was studied using a vibrating sample magnetometer (VSM). For anisotropy measurements, powders of alloys 1 and 2 were oriented in the plane of the substrate at 2.5 T and magnetization measurements were made both in easy and hard directions. The metallurgical investigations were carried out using X-ray diffraction and metallographic techniques (Optical, SEM & EPMA).

3. Results and discussion

3.1. Magnetic and thermomagnetic studies

Shown in Fig. 2 and Fig. 3 are the temperature variation of magnetization and the second quadrant hysteresis plots (normal and intrinsic) of fully heat-treated samples of ternary (sample 1) and multi-component (sample 2) NdFeB alloys. From these figures it can be seen that even though the energy product of sample 2 is nearly the same as that of sample 1, a significant improvement in coercivity (from 720 to 1000 kA/m) and Curie temperature (from 585 to 705 K) has been obtained in sample 2 and is attributed to the favourable effects of alloying additions. The effect of step aging from 875 to 675 K on the intrinsic coercivity (H_{ci}) of the samples is shown in Fig. 4. The peak coercivity is reached in sample 1 in the first stage of post-sintering heat treatment, i.e. at 875 K/1 h and further heat treatment is found to have less effect on the property enhancement. On the other hand, in sample 2, improvement in coercivity is observed with step-wise heat treatment, reaching a peak value at around 775 K.

In Fig. 5 is shown the magnetization plots of both the samples, and it can be seen by extrapolation that

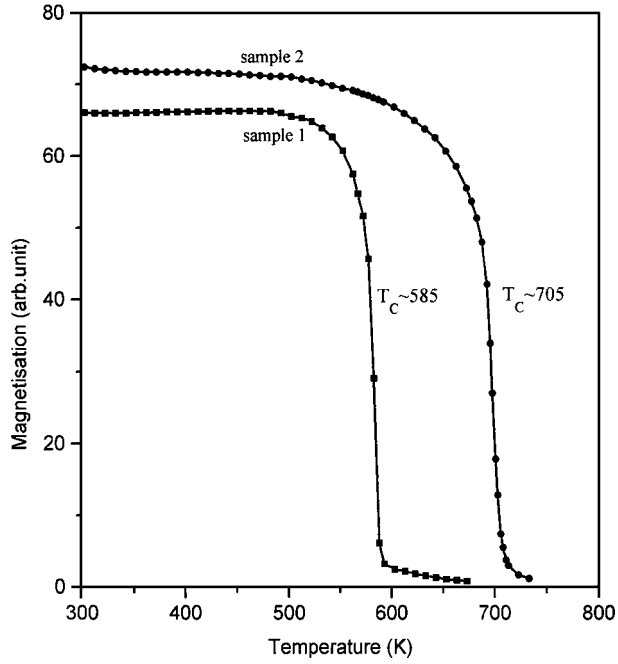

Figure 2 Temperature variation of magnetization of samples1 and 2 (bias field: 16 kA/m).

the anisotropy field H_A of the sample 2 is higher than that of sample 1.

3.2. Structural and microstructural studies

X-ray diffractograms of the sintered samples 1 and 2 (Fig. 6) show $Nd_2Fe_{14}B$ (φ) as the major phase. The maximum intensity lines (105) and (006) indicate a strong [001] grain texture development of the φ-phase.

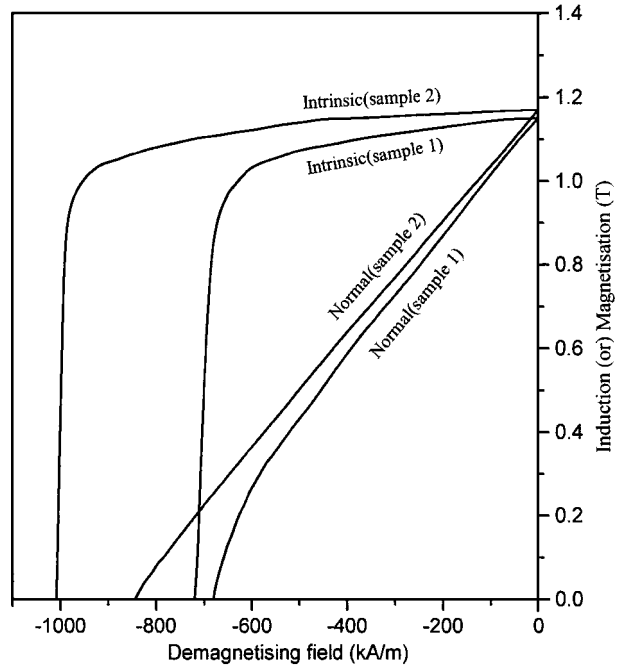

Sample No.	Magnetic properties			
	B_r (T)	H_c (kA/m)	H_{ci} (kA/m)	$(BH)_{max}$ (kJ/m^3)
1	1.15	680	720	240
2	1.17	840	1000	250

Figure 3 Second quadrant hysteresis plots of sintered and fully heat treated samples 1 and 2 (Magnetizing field: 2.0 T).

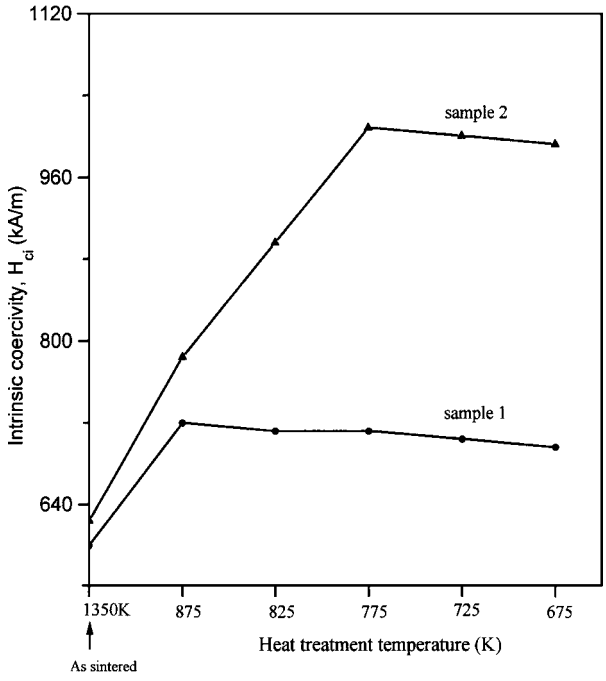

Figure 4 Plot of intrinsic coercivity versus heat treatment temperature of sintered samples 1 and 2.

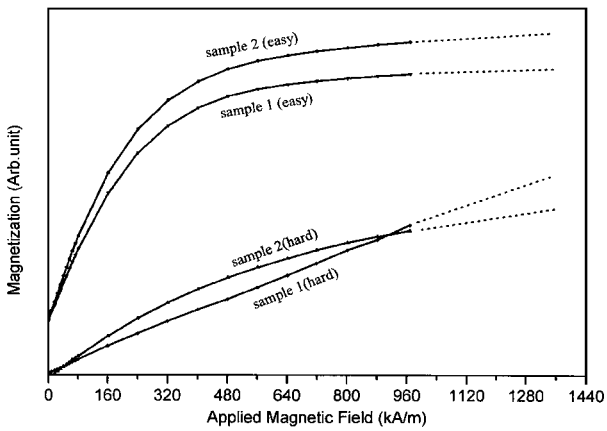

Figure 5 Magnetization plots of oriented powder of alloy 1 and 2, measured along the easy and hard axis. On extrapolation of the curves, it can be noticed that sample 2 is more anisotropic than sample 1.

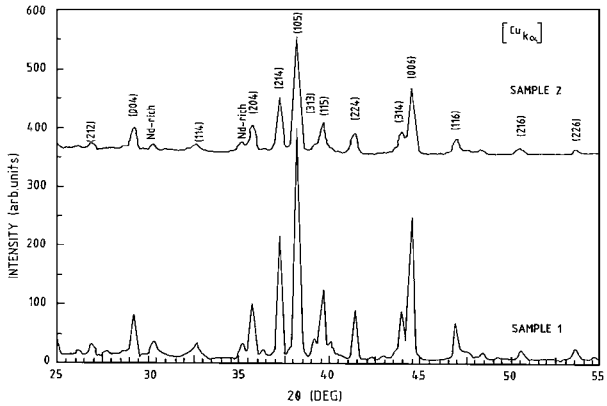

Figure 6 X-ray diffractograms taken on the surface of the samples perpendicular to the direction of magnetic orientation (*c*-axis).

The optical micrograph and the back scattered electron image of both the samples (Fig. 7) exhibit a multiphase microstructure with φ as the matrix phase. Minor phases such as $Nd_{1.1}Fe_4B_4$ (η-phase) and Nd-rich are

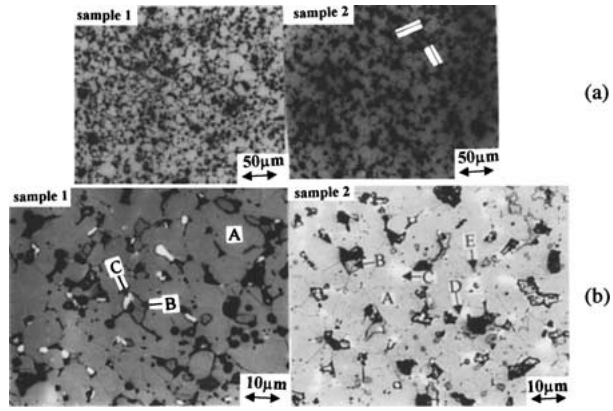

Figure 7 (a) Optical micrograph of samples 1 and 2. Fine particles (1–2 μm) of Nb-Fe rich phase distributed within the grains of φ-phase and at the grain boundary are indicated by the arrow marks. (b) SEM back scattered electron image of sample 1 and 2. Both samples display multiphase microstructure. A-$Nd_2Fe_{14}B$ (φ), B-$Nd_{1.1}Fe_4B_4$ (η), C-Nd-rich, D-Nd-oxide, E-NbFeB particles.

also found in both the samples. The presence of an additional phase in the form of tiny particles (1–2 μm) distributed inside the grain and at the boundary as well is observed in sample 2. From the EDX spectrum (Fig. 8) and the EPMA results (Table I), these particles are identified as $Nb_{13}(FeCo)_{20}B_{67}$ with a little amount of Nd soluble in it. In an earlier investigation of Nb substitution in NdFeB, Parker *et al.* [14] reported that Nb increases the coercivity and attributed this effect to the perturbation caused by these Nb-rich particles to the domain wall motion. The later studies on the role of Nb in NdFeB indicated that an hexagonal phase of NbFeB is found distributed in the grains of φ phase [15] and the formation of Nb-Fe rich phase suppresses the precipitation of Fe, whose soft magnetic nature is detrimental to the development of high coercivity [11]. Therefore, it is viewed that the formation of $Nb_{13}(FeCo)_{20}B_{67}$ is beneficial to the development of high coercivity in sample 2.

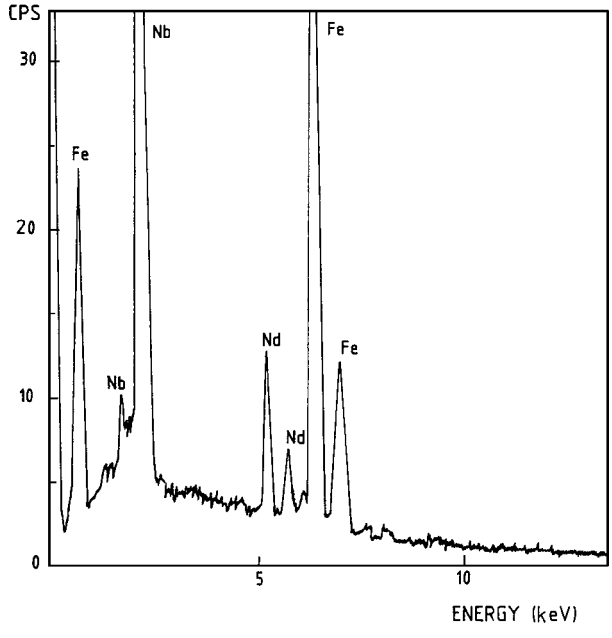

Figure 8 EDX spectrum of the fine particles found in sample 2.

TABLE I Electron Probe Microanalysis of sintered and heat-treated multi-component NdFeB magnet (sample 2)

Region analyzed	Concentration of the elements in at.%							Phase identified
	Nd	Dy	Fe	Co	Cu	Ga	Nb	
A	11.5	1.7	75.2	7.9	0.3	0.4	0.1	φ-phase
B	12.6	1.4	40.3	4.2	0.1	0.1	–	η-phase
C	51.4	0.5	3.0	8.1	27.6	8.6	–	(NdDy)(CuGaCoFe)
D	28.0	1.9	1.5	0.3	0.1	–	–	(NdDy)(FeCo)-Oxide
E	0.3	–	18.3	1.7	0.1	–	12.7	$Nb_{13}(FeCo)_{20}B_{67}$

It is further seen from Fig. 7 that the Nd-rich phase is distributed mostly at the grain junctions, overlapping the pores, partly or wholly, and extending into the grain boundary region. This phase appears in two forms in sample 2 with differentiating contrast as shown in Fig. 9a. The EDX spectrum (Fig. 9b) indicates that the Nd-rich region with bright contrast exhibits solubility of the dopant elements viz. Ga, Cu & Co while that of the Nd-rich phase with grey contrast (Fig. 9c) contains oxygen to the extent of ∼70 at.% and is likely to exist in the form of Nd_2O_3. The hard boride η-phase, which is identified through its dark boundary, is seen in samples 1 and 2 as separate grains, distributed at the grain junctions and at the intergranular regions. A reduction in the size and volume fraction of this phase is noticed in sample 2, which is considered beneficial for the enhancement of the magnetic properties. A schematic representation of the distribution of the various phases observed in sample 2 is given in Fig. 10.

From the results of EPMA shown in Table I, the distribution of the dopant elements in various phases in sample 2 can be seen. Cu and Ga preferentially go into the bright Nd-rich phase, although they exhibit solubility in very low concentration level (<0.3 at.%) in the matrix phase. The phase composition as obtained from EPMA approximately corresponds to (NdDy)(FeCuCoGa) in 1 : 1 ratio. The total concentration of Cu, Ga and Co in this phase is around 50 at.% out of which 20–30 at.% is Cu. According to Ohmori [7], a change of Nd-rich phase from Nd-Fe base to Nd-Cu is accompanied by depression of melting point (from 928 K to ∼793 K). The decrease in the melting point of the Nd-rich phase has a greater influence in the uniformity of the distribution of this phase. Therefore, it is inferred from the present study that the Nd-Cu phase formed at the intergranular region is beneficial for the development of high coercivity.

Dy partitions mostly into the φ-phase, η-phase and Nd-rich (oxide) phase. The partial substitution of Dy in φ-phase is also evident from the higher anisotropy (H_A) exhibited by the multi-component alloy (sample 2) as compared to the ternary NdFeB (sample 1) with similar rare earth concentration. Dy has negligible solubility in the Nd-Cu rich phase and in the Nb-Fe rich phase. Co exhibits maximum solubility (8 at.%) in the φ-phase and in the Nd-Cu rich phase. Buschow [4] has evaluated the exchange coupling constant between 3d-3d moments and 3d-4f moments in $R_2Co_{14}B$ and $R_2Fe_{14}B$ and found that 3d-3d exchange in $R_2Co_{14}B$ is more than three times that in $R_2Fe_{14}B$. Since in the present study Co has replaced Fe, the increase in T_C can be

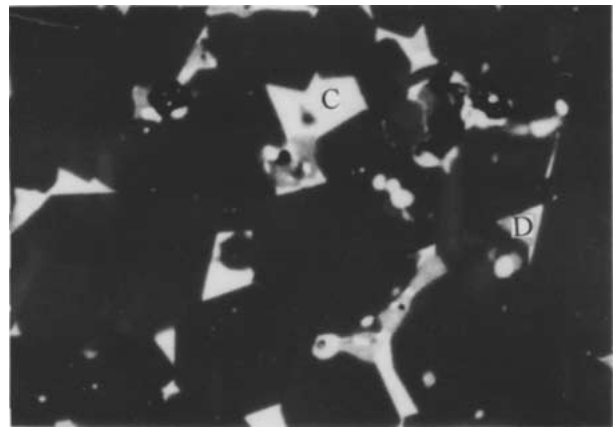

(a)

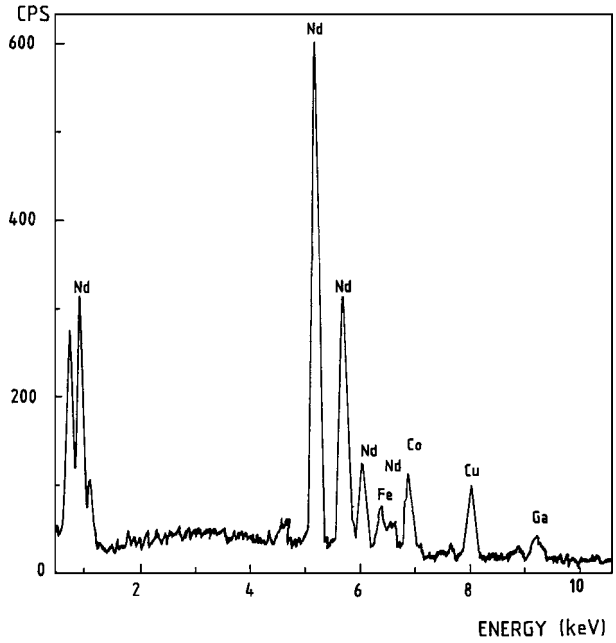

(b)

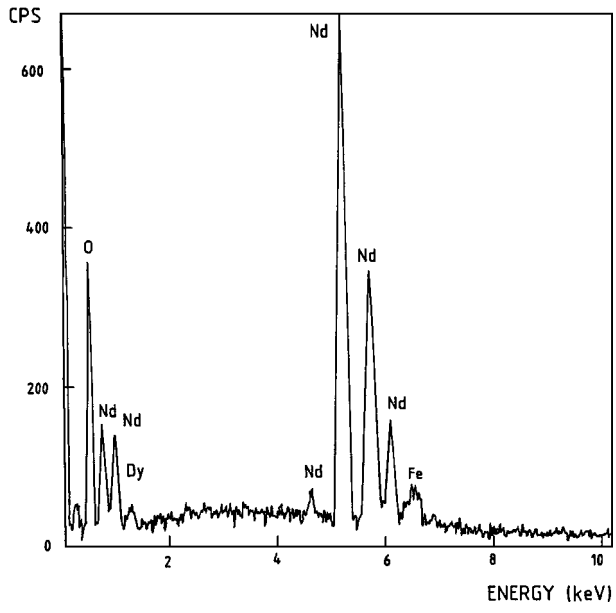

(c)

Figure 9 (a) SEM back scattered electron image showing the intergranular region in sample 2. Nd-rich phases are found in two different contrast *viz*. bright (C) and grey (D). (b) EDX spectrum of the bright intergranular phase showing the presence of Cu, Ga and Co besides Nd. (c) EDX spectrum of the grey intergranular phase showing the presence of oxygen and Nd.

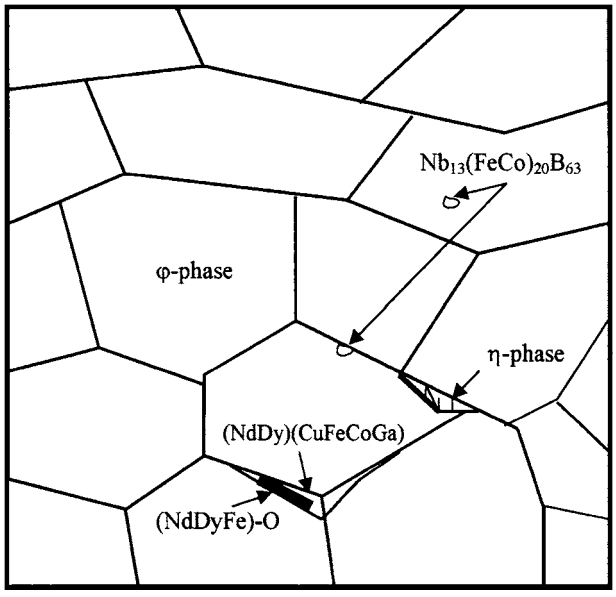

Figure 10 A schematic of the distribution of various phases in the sintered and step-aged multi-component sample 2.

attributed to the increase in the exchange between 3d-3d moments.

The solubility of Co in the other minor phases such as η-phase and $Nb_{12}(FeCo)_{21}B_{67}$ phase, is quite limited to approximately 4 at.% and 2 at.%, respectively. Least solubility of Co is shown by the Nd-rich oxide phase.

3.3. Coercivity and microstructure

The main coercivity mechanism prevailing in NdFeB magnet is of nucleation type [16]. However, domain wall pinning at the grain boundary has also been reported [17], particularly to account for the coercivity improvement in NdFeB samples containing refractory elements. The coercivity enhancement on step-wise heat treatment in sample 2 may therefore be attributed to the strengthening of the pinning sites at the grain boundary by the migration of the non-magnetic elements. Further, in sample 2 even with 8 at.% Co, soft magnetic phases such as $Nd(FeCo)_2$ and $Nd(FeCo)_3$ are not observed. The addition of Cu along with Ga seems to profoundly modify the grain boundary phase into one of non-magnetic, with depression of melting point.

Precipitation of Fe can occur in NdFeB due to non-equilibrium solidification of the alloy since a high temperature Fe freezing zone exists in the ternary phase diagram [18]. The detrimental effect of Fe particles is circumvented by the addition of Nb in small quantity, leading to the formation of boride precipitate particles of Fe-Nb.

4. Conclusions

The microstructural and magnetic investigations on the powder metallurgically processed $(Nd_{14.9}Dy_{1.9})(Fe_{65.0}Co_{8.0}Cu_{1.0}Ga_{1.0}Nb_{0.7})B_{7.5}$ alloy are summarised as follows:

1. Addition of Dy,Co,Ga,Nb and Cu results in (a) the partitioning of Dy and Co to a larger extent into the matrix phase(φ), (b) the solubility of Cu,Ga and to a lesser extent Co into the intergranular Nd-rich phase and (c) the formation of NbFeB phase, suppressing the precipitation of free Fe particles.

2. The alloy exhibits Curie temperature of 705 K and the improvement as compared to ternary system is attributed to the large solubility of Co in φ-phase.

3. The realisation of high intrinsic coercivity (1000 kA/m) is attributed to (a) solubility of Dy in φ-phase leading to increase in H_A (b) better distribution of the sintering aid liquid phase owing to decrease in the melting temperature caused by dopant elements (Ga and Cu) and (c) suppression of Fe precipitation by the addition of the refractory element (Nb). A multi stage step-wise post sintering heat treatment helps in achieving this property.

Acknowledgements

The authors gratefully acknowledge the support rendered by DRDO in carrying out this work. S. Pandian and V. Chandrasekaran wish to thank the Director, DMRL for his encouragement to publish this research work. The support received from Mr. ML Patel, the Group Head, MMG, DMRL is gratefully acknowledged. Thanks are due to Dr. Markendeyulu, IIT, Madras for the helpful discussions.

References

1. D. LI, H. F. MILDRUM and K. J. STRNAT, *J. Appl. Phys.* **57**(1) (1985) 4140.
2. E. B. BOLTICH, E. OSWALD, M. Q. HUANG, S. HIROSAWA, W. E. WALLACE and E. BURZO, *ibid.* **57**(1) (1985) 4106.
3. K. FRITZ, J. GUTH, B. GRIEB, E-THEO HENIG and G. PETZOW, *Z. Metallkd.* **83** (1992) 791.
4. K. H. J. BUSCHOW, D. B. DE MOOIJ, S. SINNEMA, R. J. RADWANSKI and J. J. M. FRANSE, *J. Magn. & Magn. Mater.* **51** (1985) 211.
5. H. YAMAMOTO, S. HIROSAWA, S. FUJIMURA, K. TOKUHARA, H. NAGATA and M. SAGAWA, *IEEE Trans. Magn.* **MAG-23** (1987) 2100.
6. M. SAGAWA and S. HIROSAWA, *J. Mater. Res.* **3**(1) (1988) 45.
7. K. OHMORI, LIN LI and C. D. GRAHAM, JR., *IEEE Trans. Magn.* **MAG-28** (1992) 2139.
8. M. TOKUNAGA, H. HARADA and S. R. TROUT, *ibid.* **MAG-23** (1987) 2284.
9. B. GRIEB, C. PITHAN, E.-TH. HENIG and G. PETZOW, *J. Appl. Phys.* **70**(10) (1991) 6354.
10. C. H. LIN, C. J. CHEN, C. D. WU, W. C. CANG, S. K. CHEN and T. S. CHIN, *IEEE Trans. Magn.* **MAG-26** (1990) 2607.
11. W. L. LIU, Y. L. LIANG, B. M. MA and C. O. BOUNDS, *ibid.* **MAG-28** (1992) 2154.
12. J. Q. XIE, C. H. WU, Y. C. CHUANG and F. M. YANG, *J. Appl. Phys.* **68**(8) (1990) 4208.
13. M. TOKUNAGA, H. KOGURE, MENDOH and H. HARADA, *IEEE Trans. Magn.* **MAG-23** (1987) 2287.
14. S. F. H. PARKER, R. J. POLLARD, D. G. LORD and P. J. GRUNDY, *ibid.* **MAG-23** (1987) 2103.
15. P. SCHREY, *J. Magn. & Magn. Mater.* **73** (1988) 260.
16. H. KRONMÜLLER, *MRS Intl. Mtg. on Adv. Mater.* **11** (1989) 3.
17. G. C. HADJIPANAYIS, K. R. LAWLESS and C. DICKERSON, *J. Appl. Phys.* **57**(1) (1985) 4097.
18. G. SCHNEIDER, E.-THEO HENIG, G. PETZOW and H. H. STADELMAIER, *Z. Metallkd.* **77** (1986) 755.

Received 6 July 2000
and accepted 3 August 2001